jh190072-NAJ

State following of amorphous soft condensed matters : developments of high-performance computational schemes

Hajime Yoshino (Osaka University)

概要

The concept of jamming has attracted great research interest due to its broad relevance in soft-matter such as liquids, glasses, colloids, foams, and granular materials, and its deep connection to the sphere packing problem and optimization problems. Here we show that the domain of amorphous jammed states of frictionless spheres can be significantly extended, from the well-known jamming-point at a fixed density, to a jamming-plane that spans the density and shear strain axes.

1　共同研究に関する情報

1.1　共同研究を実施した拠点名

大阪大学サイバーメディアセンター

1.2　共同研究分野

■超大規模数値計算系応用分野

1.3　参加研究者の役割分担

- Hajime Yoshino (Cyberemedia Center, Osaka Universiry): Developement of computational scheme, data analysis
- Yuliang Jin (Institude of Theoretical Physucs, Chinese Academy of Science): Developement of computational scheme, data analysis
- Yue Deng (Institude of Theoretical Physucs, Chinese Academy of Science): Developement of computational scheme, data analysis

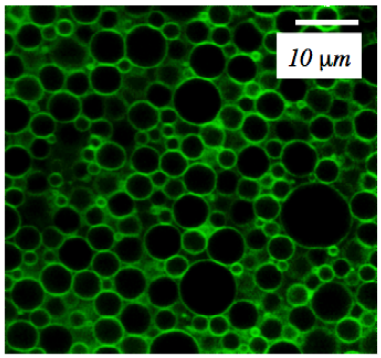

Dense assembly of emusion(cocecane droplets Immerdesd in water+glycerol, confocal microscopic Image taken by ER Weels and C Hollonger) (E. Weeks "Soft jammed materials" (2014))

2　研究の目的と意義

The purpose of this project is to develop a set of high-performance computational schemes to study rheological properties of amorphous solid states of soft-matter such as dense assemblies of colloids and emul-

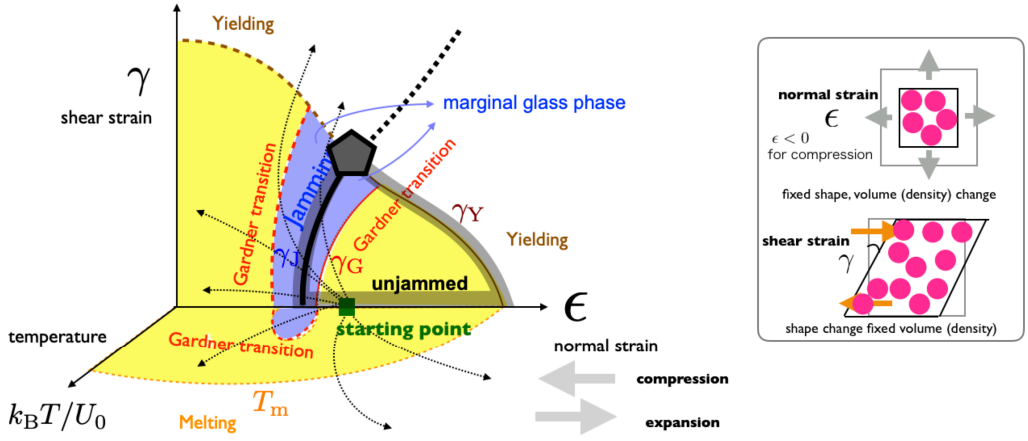

Schematic stability-map of ultra-stable, emulsion glass upon deformations (normal/shear strain) and heating: the initial glass (marked by the green square) is prepared with the help of the swap-Monte Carlo method. The region enclosed by the thick-gray line corresponds to the hard-sphere regime.

図 1

sions (see the figure above). Our project is motivated by the recent developments of the mean-field theory for amorphous, glassy soft-matters in recent years [1] which produced interesting predictions on the rheological properties [2, 3, 4]. However the mean-field theory is exact only in the large dimensional limit and its validity in the real three dimensional systems is a totally open question.

In the present project we will develop parallelized simulation schemes which enable

1. **Preparation of ultra-stable glassy states** at low temperatures/high densities. Such a state is represented as the 'starting point' - the green-square point - in Fig. 1. This is a hard-sphere configuration in a glassy state.
2. **Glass state following under quasi-static perturbations** As shown in Fig. 1, we explore the system under perturbations by applying the volume strain ϵ, shear-strain γ and temperature T. (k_B is the Boltzmann's constant.) Here U_0 is the energy scale for the deformation of spheres so that $U_0 \to \infty$ in the hard-spheres. With the hard-spheres, we are confined in the $k_BT/U_0 = 0$ plane. Starting from the initial configuration (green-square), we can bring the assembly of hard-spheres to each point in the region bounded by the thick-gray line. The hard-sphere glass state yields beyond the yielinding line γ_Y and jamms approaching shear-jamming line γ_J.

The core part of our project is **parallelization of the swap Monte Carlo (MC) [5] method** which enables preparation of "ultra-stable glasses" , i.e. unprecedentedly stable glasses against decompression and shear deformations, by computer simulations. We

then apply the scheme to elucidate rheological properties of dense assembly of emulsions.

3 当拠点公募型研究として実施した意義

After the JHPCN project, the scientific program is now smoothly continued using the same facility (OCTOPUS, Cybermedia center) by the same international team. We experienced difficult time due to over-clouding of the facility but the situation have improved after introduction of a new job class dedicated for program testing.

4 今年度の研究成果の詳細

4.1 GPU parallelization of the FIRE algorithm and the swap algorithm

In our project, the key algorithms are 1) swap Monte Carlo algorithm, 2) event-driven molecular dynamics algorithm, 3) FIRE algorithm.

This year we succeeded a GPU parallelization of the 3) FIRE algorithm [6] which allows us to follow quasi-static evolution of assemblies of soft, deformable particles under perturbations. This algorithm is used in the athermal system (strictly $T = 0$ system) under perturbations discussed in sec 4.2.2.

We are currently working on GPU parallelization of the 1) swap Monte Carlo algorithm. Swap algorithm allows very efficient thermalization of *poly-disperse* hard-sphres [5]. The single step of the swap Monte Carlo in the conventional version [5] goes as the following. i) One picks up a pair of spheres (which have different radii) randomly among the all N spheres in the system. ii) Then one tries to swap the positions (the center of mass coodinates) of the two hard-spheres. This is accepted if the new configuration do not create overlaps between the spheres with their neighbors. Otherwise the new configuration violates the hard-sphere constraint so that it is rejected. The non-local motions of the particles are, of course, artificial processes which do not exist in nature. But this greatly facilitates thermalization of the system so that it is very useful for our project which needs preparation of stable, well annealed initial configuration (green-point in Fig. 1).

The original algorithm [5] allow long-distance movement of the particles which cannot be parallelized easily. To overcome this difficulty we modified the algorithm using the standard cell decomposition technique. We divide the whole system into cells (grids) such that only a few particles are contained in each cell. Then for the swap process, we only allow exchange of the particles between adjacent cells. Then the procedure can be easily parallelized. In this modified version, particles do not make long-distance motions allowed in the original version but still make non-local motions. Currently we are trying to evaluate efficiency of the modified and parallelized algorithm comparing it with the conventional version.

4.2 Analysis of jamming

For the scientific part, this year we focused on the shear-jamming (SJ) line $\gamma_{\rm J}$, i. e. the thick and dotted black-lines in Fig. 1. For a given hard-sphere glass state, represented by the green point in Fig. 1 at density $\varphi_{\rm eq}$, there is a corresponding SJ-line along which we

find *jammed* configurations associated with the starting configuration.

Jamming is sometimes called as *random close packing* (RCP). Before explaining RCP, let us explain *close packing* (CP) which is the crystalline counterpart of RCP. The notion *close packing* refers to the maximally packed, densest configuration of simple spheres. For instance it is known in three dimensions, the densest packings of equal-sized spheres are the face-centered cubic (FCC) or the hexagonal close packing (HCP) lattices, whose densities (packing fractions) are $\varphi_{\rm FCC} = \varphi_{\rm HCP} \simeq 0.74$. For an assembly of ideal spherical equal-sized colloids, this is the ideal densest state. In this state, a colloid cannot move around at all being in direct contact with its 12 neighbours. Note that FCC crystalline state itself exist at large enough densities $\varphi > 0.49$ but the system is *not jammed* at densities below 0.74, i. .e. spheres are surounded by the 12 neighbours but they can still make rattling motions inside the cages bounded by the neighbours. Indeed the colloidal crystalline state is the thermodynamically state state at large densities $\varphi > \varphi_{\rm m} = 0.58$ because of the rattling motion: the crystalline state create larger free-volumes around spheres than disorderd liquid configurations at large enough densities so that the it is entropically more favorable than liquid at large enough densities.

The notion *jamming* or *random close packing* referes to the amorphous version of the close packing [7]. At $\varphi > 0.49$, the crystalline state emerges but the disordered, liquid state can also remain. Such a liquid state for $\varphi > \varphi_{\rm m} = 0.58$ is called as supercooled liquid state which is a metastable state. By compressing the metstable liquid state up to larger densities, the relaxational dynamics of the system becomes extremely slow leading to rapid the increase of the viscocity. At large enough densities the time scale of relaxation become so large such that the system appear as an amorphous solid state within the experimental time scale. This is the colloidal glass state. In a glass state, spheres can still make rattling motinos inside cages created by the neighbours. Now compressing the system further, at a certain point the system *jamms*. It is known that in the amorhous jammed states of friction-less simple spheres, a sphere is surounded on average by 6 neighbours.

The amorphous jammed state is very different from the crystalline CP state in several respects. First it is only *marginally* stable in the mechanical sense. The average contact number 6 is the minimum number of contact below which the mechanical force balance between the spheres cannot be maintained. The situation is called as *isostatic*. Second, the jamming density $\varphi_{\rm j}$ is *not* unique but depends on the details of the preparation protocols in sharp contrast to the crystalline CP which has $\varphi_{\rm CP} \simeq 0.74$. Thus a very interesting question is to what extent the jammed states share common, universal properties.

Spheres can be constrained not only by compression but also by shear. In granular rheology, the volume (in isobaric processes) or the pressure (in isovolumetric processes) of an assembly of granular particles can increase under shear, known as Reynolds dila-

tancy [8]. Indeed granular matter and suspensions can be jammed by shear. However, previous studies found that, for frictionless spheres, shear jamming and isotropic jamming occur at the same, γ independent density in the thermodynamic limit [9]. We show that this is not true in general (see Fig. 2). In the following report our results on jamming explored by compression and shear (Jin-Yoshino, 2020).

4.2.1 Models

The systems consist of N spherical particles in a simulation box of volume V, with a continuous diameter distribution $P(D) \sim D^{-3}$, where $D_{\min} \leq D \leq D_{\min}/0.45$ [5]. The number density is $\rho = N/V$ and the volume fraction is $\varphi = \rho(4/3)\pi\overline{D^3}$. The mean diameter $\overline{D}$ is set as the unity of length, and all particles have the same unit mass $m = 1$. For the same $P(D)$, two models are studied.

(i) **Thermal hard sphere (HS) model**. The model represents a suspension of hard colloidal particles with negligible friction. The simulation is performed under constant unit temperature $T = 1$. Because the potential energy is always zero and only inter-particle collisions contribute, both pressure $P_{\rm entro}$ and stress $\Sigma_{\rm entro}$ are purely *entropic*. We define the reduced entropic pressure as $p_{\rm entro} = P_{\rm entro}V/Nk_{\rm B}T$ and the reduced entropic stress as $\sigma_{\rm entro} = \Sigma_{\rm entro}V/Nk_{\rm B}T$, and set the Boltzmann constant $k_{\rm B} = 1$. The method to compute $p_{\rm entro}$ and $\sigma_{\rm entro}$ is explained in detail in Ref. [10]. Jamming occurs when the entropic pressure and stress diverge.

(ii) **Athermal soft sphere (SS) model**. The model represents a frictionless granular system. The SS potential has a harmonic form $U(r_{ij}) = \frac{1}{2}(1 - r_{ij}/D_{ij})^2$ (zero if $r_{ij} > D_{ij}$), where r_{ij} is the inter-particle distance between particles i and j, and $D_{ij} = (D_i + D_j)/2$ is the mean diameter. The simulation is performed at zero temperature. Both pressure $P_{\rm mech}$ and stress $\Sigma_{\rm mech}$ are contributed by the mechanical contacts between particles, and therefore are purely *mechanical*. The SSs are jammed if $P_{\rm mech} > 0$, and the unjamming transition occurs as $P_{\rm mech} \to 0$.

For the initial states, we generate equilibrium liquid configurations of the thermal HS model at $\varphi_{\rm eq} > 0$, as well as purely random (ideal gas) configurations at $\varphi_{\rm eq} = 0$. To use these initial configurations in the athermal protocol (sec. 4.2.2), we simply need to replace the thermalized HSs by SSs at the same positions, and switch off the temperature.

4.2.2 Athermal Protocol

Let us present here the results on jamming obtained by the athermal SS model. We used the following protocols to generate the jammed states starting from the initial glass state.

(i) **Athermal rapid compression (ARC)**. First, we instantaneously switch off the temperature of a HS equilibrium configuration at $\varphi_{\rm eq}$. We then work at zero temperature using the SS inter-particle potential. The particle

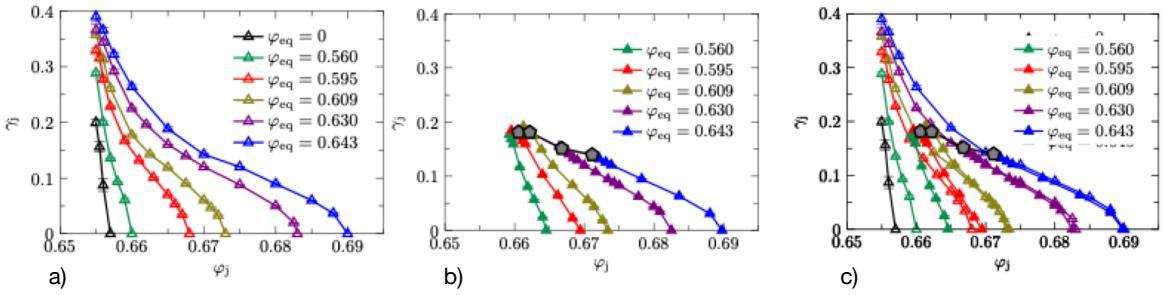

図 2 Shear-Jamming (SJ)-lines obtained by the athermal and thermal protocols. For a given hard-sphere glass state (green point in Fig. 1) at density φ_{eq}, there is a corresponding SJ-line along which we find jammed configurations associated with the starting configuration. In panel a) the SJ-lines of various φ_{eq} obtained by athermal protocol (sec 4.2.2) are displayed. In panel b), the corresponding SJ-lines obtained by thermal protocol (sec 4.2.3) are displayed. In panel c), the SJ-lines obtained by the two protocols are displayed on top of each other. Note that shear-jamming lines are *not* vertical except for the special case $\varphi_{eq} = 0$.

sizes are inflated or deflated proportionally and instantaneously to match a target density φ_j. Overlaps between particles are removed by minimizing the total potential energy using the FIRE algorithm [6].

(ii) **Athermal quasistatic shear (AQS).** If the configuration is not jammed after the previous step, we further apply AQS to the unjammed configuration. A simple shear deformation in the x-z direction is applied under Lees-Edwards boundary conditions [11]. At each step, all particles are shifted instantaneously by $x_i \to x_i + \delta\gamma z_i$, where x_i and z_i are the $x-$ and $z-$coordinates of particle i, and $\delta\gamma$ is the strain step size, followed by the FIRE algorithm to remove the overlaps.

In Fig. 2 a), we show the shear-jamming (SJ) lines obtained by the athermal protocols. The jamming without shear $\gamma = 0$ is obtained by ARC. The jamming under shear is obtained by ARS+AQS.

4.2.3 Thermal Protocol

Now we turn to jamming obtained by the thermal HS model. We used the following protocols to generate the jammed states starting from the initial glass state.

(i) **Thermal compression (TC).** To compress the thermal HS, we use the Lubachevsky-Stillinger algorithm [12], which is based on event-driven molecular dynamics. Starting from an equilibrium configuration at φ_{eq}, the algorithm compresses HSs by inflating their sizes with a fixed rate $\Gamma = \frac{1}{2D}\frac{dD}{dt}$. The simulation time is expressed in unit of $\sqrt{1/k_B m\overline{D}^2}$.

(ii) **Thermal quasi-static shear (TQS)** To simulate shear on the thermal HS, we apply constant volume simple shear in the x-z direction with a fixed rate $\dot{\gamma} = 10^{-4}$. At each step, we perform 1000 collisions per particle, and then instantaneously increase the shear strain by $\delta\gamma = \dot{\gamma}\delta t$, where δt is the time elapsed during the collisions. All particles are shifted by $x_i \to x_i + \delta\gamma z_i$. To remove the possible overlappings introduced during this shift, we switch to the SS potential and use the FIRE algorithm to minimize the energy. The SS potential is switched off after. Lees-Edwards boundary conditions are used.

In Fig. 2 b), we show the shear-jamming (SJ) lines obtained by the thermal protocols. The jamming without shear $\gamma = 0$ is obtained by TC. The jamming under shear is obtained by TC+TQS.

4.2.4 Reversibility

In Fig. 2 c), we show the shear-jamming (SJ) lines obtained by the athermal and thermal protocols together. One can see that the SJ lines of the thermal HS model obtained by the thermal protocol agrees with those of the athermal SS model obtained by the athemal protocl up to the 'pentagon'. See also Fig. 1 where we also indicated the 'pentagon' point.

We found jammed states below the 'pentagon' can be reversed back to the initial starting point (the green square in Fig. 1 in the following sense. By reversing the protocols, the configuration of the system can be brought *almost* back to the initial configuration: by measuring the mean-squared displacement (MSD) between the initial configuration and the configuration after the reversed process from the jammed states, we found very small MSD of the order of that due to thermal fluctuation inside cages of the initial, unperturbed glass states.

4.2.5 Isostaticity and Jamming Universality

We found *all* the jammed states obtained are *sostatic* (Fig. 3 (c)). The scaling properties approaching the jamming is universal in *all* cases: i) power law scaling of the energy approaching unjamming (SS) (Fig. 3 (a)), ii) power law scaling of the excess contact number and mechanical pressue above jamming (SS) (Fig. 3 (b)), and ii) power law scaling of the distribution of gap between spheres approaching jamming (HS/SS) (Fig. 3 (d)).

5 今年度の進捗状況と今後の展望

We are satisfied with the scientific progress on shear-jamming (thick and dotted black lines in Fig. 1) as reported above. As for the next step we will explore non-linear rheological properties related to yielding of athermal soft-spheres (dotted yielding line $\gamma_{\rm Y}$) in Fig. 1). The parallelization of the FIRE algorithm is satisfactory and this will also greatly help us in the analysis of the non-linear rheology.

We are continuing the assessment of the efficiency of the parallelized version of the swap algorithm compared with the conventional one. Once established this method will be very useful in studies of dense assembly of soft-matters.

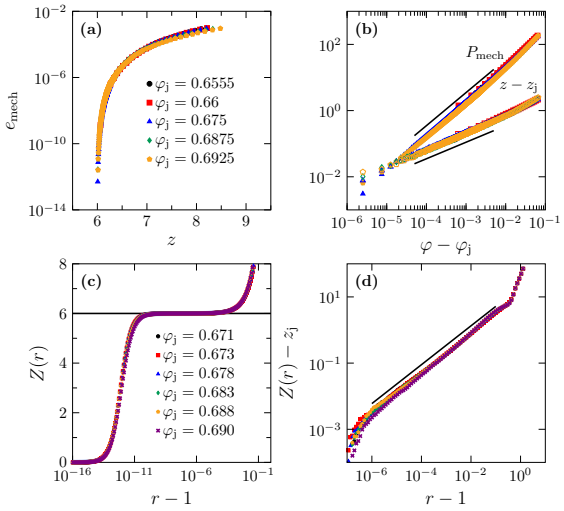

図 3　Isostaticity and universality of jamming. We show scalings (a-b) above jamming $\varphi > \varphi_{\rm j}$ in athermal SSs, and (c-d) below jamming $\varphi < \varphi_{\rm j}$ in thermal HSs, for $\varphi_{\rm eq} = 0.643$ and $N = 8000$. Data in (a-b) are obtained from athermal compressions of SS packings from $\varphi_{\rm j}$ to φ, for a few different $\varphi_{\rm j}$ along the SJ-line. (a) Energy density $e_{\rm mech}$ versus coordination number z. (b) Mechanical pressure $P_{\rm mech}$ and the excess coordination number $z - z_{\rm j}$ as functions of $\varphi - \varphi_{\rm j}$.

6　研究業績一覧（発表予定も含む）

学術論文 （査読あり）

- Yuliang Jin, Hajime Yoshino, ‘A Jamming Plane of sphere packings’, (submitted) preprint: arXiv:2003.10814

参考文献

[1] Patrick Charbonneau, Jorge Kurchan, Giorgio Parisi, Pierfrancesco Urbani, and Francesco Zamponi. *Nature communications*, 5:3725, 2014.

[2] Hajime Yoshino and Francesco Zamponi. *Physical Review E*, 90(2):022302, 2014.

[3] Corrado Rainone, Pierfrancesco Urbani, Hajime Yoshino, and Francesco Zamponi. *Physical review letters*, 114(1):015701, 2015.

[4] Pierfrancesco Urbani and Francesco Zamponi. *Physical review letters*, 118(3):038001, 2017.

[5] Ludovic Berthier, Daniele Coslovich, Andrea Ninarello, and Misaki Ozawa. *Phys. Rev. Lett.*, 116:238002, Jun 2016.

[6] Erik Bitzek, Pekka Koskinen, Franz Gähler, Michael Moseler, and Peter Gumbsch. *Physical review letters*, 97(17):170201, 2006.

[7] M. Van Hecke. *Journal of Physics: Condensed Matter*, 22:033101, 2010.

[8] O Reynolds. *Proc. R. Inst. GB*, 11(354363):12, 1886.

[9] Marco Baity-Jesi, Carl P Goodrich, Andrea J Liu, Sidney R Nagel, and James P Sethna. *Journal of Statistical Physics*, 167(3-4):735–748, 2017.

[10] Yuliang Jin and Hajime Yoshino. *Nature Communications*, 8, 2017.

[11] AW Lees and SF Edwards. *Journal of Physics C: Solid State Physics*, 5(15):1921, 1972.

[12] Monica Skoge, Aleksandar Donev, Frank H Stillinger, and Salvatore Torquato. *Physical Review E*, 74(4):041127, 2006.